

Dioxygen bond scission and haem degradation in haemproteins: a kinetic study of chemical model systems using ferrimyoglobin and haempeptide:non-haempeptide complexes as catalysts for 'peroxidasic' reduction of hydrogen peroxide

Paul A. Adams* and Judith Louw

MRC Biomembrane Research Unit, Department of Chemical Pathology, University of Cape Town Medical School, Observatory 7925, South Africa

Ferrimyoglobin (Fe^{3+}Mb) and the haempeptide:non-haempeptide (HP:NHP) non-covalent complex 1-50:51-104 derived from cytochrome c, have been utilized to investigate factors directing the mechanism of -O-O- bond scission in haemprotein redox enzymes, and those affecting haem degradation or haem protection in these proteins.

The kinetic mechanism for the 'peroxidasic' reduction of H_2O_2 by these catalysts is established using diammonium 2,2'-azinobis(3-ethylbenzothiazoline-6-sulfonate) (ABTS) as reducing substrate. The effect of Br^- and HCO_2^- ions on the kinetics of the Fe^{3+}Mb reaction indicates that dioxygen bond scission in this system does result in some formation of hydroxyl radicals, *i.e.* the reaction has a homolytic component.

The effect of pH on the kinetics of H_2O_2 reduction and haem degradation is reported, and the dimensionless ratio of efficiencies for sequential reaction is proposed as a useful parameter for assessment of haem degradation. It is shown that the 'alkaline' transition in the HP:NHP complex could reflect formation of a catalytically inactive hydroxo-complex.

Introduction

An important aspect of structure-function studies of the haemproteins concerns the use of chemical model systems to mimic specific aspects of haemprotein reactivity in a more controllable and variable chemical environment than that attainable using the haemproteins themselves.

Many haemproteins utilize ferriprotoporphyrin IX—haemin—(or close chemical analogues thereof) for the whole of their varied reactivity, and haem complexes therefore form an ideal subject for this type of model study. Investigations into both O_2 transport and redox reactivity have been made using a range of haemin derivatives specifically designed to include structural features thought to be relevant to protein function and these studies have been extensively reviewed.^{1,2}

We have been particularly interested in the use of ferriprotoporphyrin IX, and more recently the small haempeptides derived from cytochrome c—the microperoxidases (abbreviated, MP-s), as chemical models of haemprotein redox catalytic activity (modelling the peroxidase and cytochrome P-450 enzymes) and, in using the MP-s as models for monomeric haemin to study the kinetic mechanism of haem-protein interaction processes in aqueous solution.³⁻⁵ Physio-chemical factors of particular interest concerning the redox catalytic activity of haemprotein models are the nature of -O-O- bond cleavage (*i.e.* homolytic or heterolytic) in the peroxidasic reduction of H_2O_2 ; haem degradation during the catalytic process, and the manner in which the 'environment' and accessibility of the haem within the protein affects both catalytic mechanism and haem degradation.

In the study reported here we characterize ferrimyoglobin— Fe^{3+}Mb —as a monomeric model for the 'peroxidasic' reduction of H_2O_2 using ABTS as reducing substrate. It is thought that -O-O- bond cleavage in the Fe^{3+}Mb catalysed reduction could proceed by parallel heterolytic and homolytic mechanisms⁶ (the latter having been originally proposed by George⁷) this possibility could be tested using the procedure suggested by Rush and Koppenol⁸ whereby the effect of Br^- and HCO_2^-

ions on the efficiency of ABTS^{*+} formation can be utilized to indicate the intermediacy of OH^\cdot radicals—this would be the first product of heterolytic dioxygen bond scission prior to protein radical formation.⁶ Furthermore, the haem is enfolded by a highly ordered and stable protein structure which should physically shield the tetrapyrrole ring system of the haem from degradative attack by oxidising species during catalytic cycling in the presence of ABTS.

The second complementary model system investigated here is the haempeptide:non-haempeptide, non-covalent complex (abbreviated, HP:NHP) comprising the haempeptide fragment 1-50 and non-haempeptide fragment 51-104, prepared by acid cleavage of the peptide bond between amino acid residues 50 and 51 of cytochrome c. This complex is one of a range of such highly stable compounds prepared by chemical digestion or semisynthetic techniques from native cytochrome c, and extensively studied by Wallace and co-workers with respect to biological electron transport activity.⁹ At a low pH these complexes exhibit a 695 nm absorbance band characteristic of an intact cytochrome c haem crevice with fifth and sixth ligands of the iron being derived from His-18 and Met-80 of the protein amino acid sequence, respectively. The 'alkaline transition' for the disappearance of this band in the HP:NHP used here has a $\text{p}K_a$ of ≈ 7.35 indicating that the methionine- Fe^{3+} bond is far weaker in this complex than in cytochrome c ($\text{p}K_a = 9.30$), a conclusion also supported by the redox properties of the HP:NHP relative to cyt-c.¹⁰ It has been argued¹⁰ that haem cleft disruption results from hydrogen bond breakage and increased solvent penetration of the haem environment, this HP:NHP complex should thus provide a useful model to assess the effect of the polarity of the environment of the haem distal face on redox catalysis in the pH range 5-9 studied here. In addition, comparison of the HP:NHP with Fe^{3+}Mb a protein of similar size, but which does not exhibit any significant structural changes with regard to the environment of the haem distal face in the pH range 6-8, and with the smaller haem peptides (MP-8 and MP-11) in which the haem distal face is (in

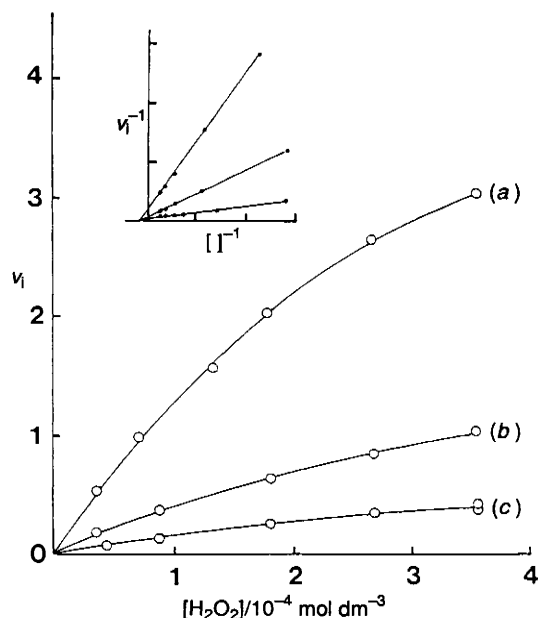


Fig. 1 Hyperbolic dependence of $v_i \equiv (d[\text{ABTS}^{*+}]/dt)_{t=0}$ on $[\text{H}_2\text{O}_2]$ at three concentrations of Fe^{3+}Mb {4.76 (a); 0.82 (b) and 0.41 (c) $\times 10^{-6}$ mol dm^{-3} , $[\text{ABTS}] = 1 \times 10^{-3}$ mol dm^{-3} }. The inset to the figure shows double reciprocal plots of the data, these visually demonstrate the hyperbolic dependence with an essentially invariant $K_{m(\text{app})}$. The units of v_i are 10^7 mol dm^{-3} s^{-1} .

the monomer) fully exposed to bulk solvent at all pH values, was a further major objective of these studies.

Results

Initial studies focussed on the characterization of the macroscopic steady-state, and non-saturation kinetic properties of the two systems, the results of these investigations will be briefly presented in order to provide a basis for the mechanistic/degradative studies and for direct comparison with the MP-8- H_2O_2 -ABTS system reported previously.⁴

The system $\text{Fe}^{3+}\text{Mb}-\text{H}_2\text{O}_2$ -ABTS

The kinetic results obtained at pH 7.00 and $(25.0 \pm 0.02)^\circ\text{C}$ under the concentration conditions $[\text{ABTS}] \gg [\text{Mb}]$ are summarized as follows.

Initial rates (v_i) of ABTS^{*+} formation were directly proportional to $[\text{Mb}]$ at constant $[\text{H}_2\text{O}_2]$ and $[\text{ABTS}]$; independent of $[\text{ABTS}]$ at constant $[\text{Mb}]$ and $[\text{H}_2\text{O}_2]$ and varied hyperbolically with $[\text{H}_2\text{O}_2]$ at constant $[\text{ABTS}]$ and $[\text{Mb}]$ (Fig. 1 and inset). The three data sets of Fig. 1 plus two further data sets not shown were accurately modelled by a saturation type equation of the form (1), with $K_m = (5.9 \pm 0.4$

$$v_i = \frac{V_{\text{max}}[\text{H}_2\text{O}_2]}{K_m + [\text{H}_2\text{O}_2]} \quad (1)$$

$\text{SD}) \times 10^{-4}$ mol dm^{-3} and $V_{\text{max}}/(K_m \times [\text{Mb}]) = 421 (\pm 35 \text{SD})$ dm^3 mol^{-1} s^{-1} , in the Fe^{3+}Mb concentration range $4 \times 10^{-7} \leq [\text{Fe}^{3+}\text{Mb}] \leq 8 \times 10^{-6}$ mol dm^{-3} .

Under the concentration conditions $[\text{H}_2\text{O}_2] \ll K_m$ concentration-time profiles for ABTS^{*+} formation were accurately represented by a general first-order integrated rate equation (see Experimental section) to $>95\%$ reaction extent. Prediction of the absorbance value at infinite time from fitting of absorbance-time data obtained in the region 0–80% reaction under the $[\text{H}_2\text{O}_2]$ restriction above, typically gave results agreeing with the experimentally observed infinity value, to

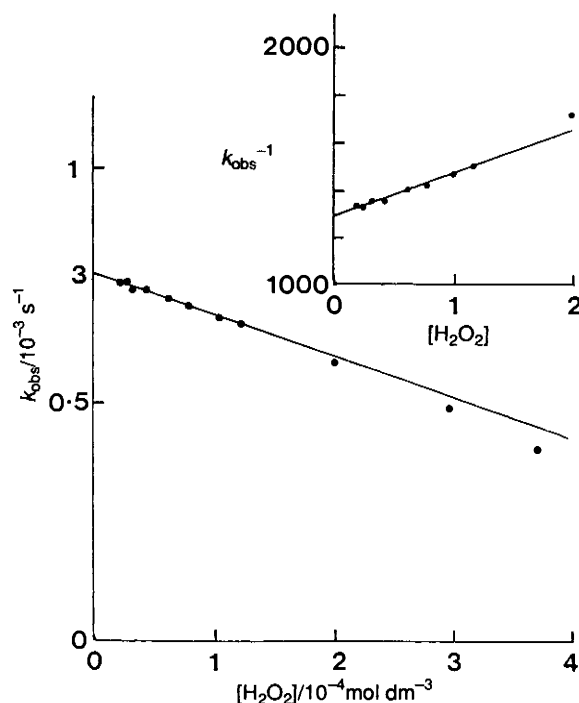


Fig. 2 $[\text{H}_2\text{O}_2]$ dependence of k_{obs} for the Fe^{3+}Mb system at constant $[\text{ABTS}] = 1 \times 10^{-3}$ mol dm^{-3} and $[\text{Fe}^{3+}\text{Mb}] = 1.59 \times 10^{-6}$ mol dm^{-3} . The slope and intercept of the limiting straight line (as $[\text{H}_2\text{O}_2] \rightarrow 0$; i.e. $\ll K_{m(\text{app})}$) are (from ref. 11) V_m/K_m^2 and V_m/K_m . $[\text{Mb}] = 1.49 \times 10^{-6}$ mol dm^{-3} . From the Fig. $K_m = 6.8 \times 10^{-4}$ mol dm^{-3} and $V_m/(K_m \times [\text{Mb}]) = 485$ mol^{-1} dm^3 s^{-1} .

better than 0.5%. Pseudo first-order kinetic studies on the Fe^{3+}Mb system were thus carried out at $[\text{H}_2\text{O}_2] < K_m/30$. Under these conditions the first-order rate constant evaluated lies within 2% of the 'true' value for k , namely V_m/K_m ,¹¹ in addition this difference is constant for all runs, thus variations observed for k accurately reflect those shown by V_m/K_m .

At constant $[\text{ABTS}]$ and $[\text{Fe}^{3+}\text{Mb}]$, k_{obs} varied with $[\text{H}_2\text{O}_2]$ as shown in Fig. 2. This behaviour is precisely that expected from a kinetic system of the Michaelis Menten catalytic type under steady state condition with respect to the catalyst-substrate complex (as the ratio $[\text{H}_2\text{O}_2]/K_{m(\text{app})} \rightarrow 0$) (inset to Fig. 2), and in the absence of substrate mediated catalyst degradation.¹¹

Under the same pseudo first-order restriction k_{obs} was found to be independent of $[\text{ABTS}]$ but directly proportional to $[\text{Fe}^{3+}\text{Mb}]$ (Fig. 3). The apparent second-order rate constant calculated from the variation in k_{obs} with $[\text{Fe}^{3+}\text{Mb}]$ was (390 ± 12) dm^3 mol^{-1} s^{-1} .

Difference spectroscopy in the Soret region of the spectrum at $[\text{ABTS}]$ up to 1×10^{-2} mol dm^{-3} revealed no evidence of complex formation between Fe^{3+}Mb and ABTS.

The system HP:NHP-ABTS- H_2O_2

The following aspects of the kinetics exhibited by this system directly parallel those found for the MP-8 catalysed process.⁴

(i) At constant $[\text{ABTS}]$ the initial rates of ABTS^{*+} formation were directly proportional to $[\text{HP:NHP}]$ at constant $[\text{H}_2\text{O}_2]$ and *vice versa*, in the concentration ranges $[\text{HP:NHP}] \leq 3 \times 10^{-6}$ mol dm^{-3} ; $[\text{H}_2\text{O}_2] \leq 2 \times 10^{-4}$ mol dm^{-3} with $[\text{H}_2\text{O}_2] \gg [\text{HP:NHP}]$. The system is thus undergoing catalytic turnover with $[\text{H}_2\text{O}_2] \ll K_{m(\text{app})}$. In agreement with this observation ABTS^{*+} formation follows precise pseudo first-order kinetics, in the concentration ranges used, for $>95\%$ reaction.

(ii) k_{obs} for ABTS^{*+} formation shows positive slope straight

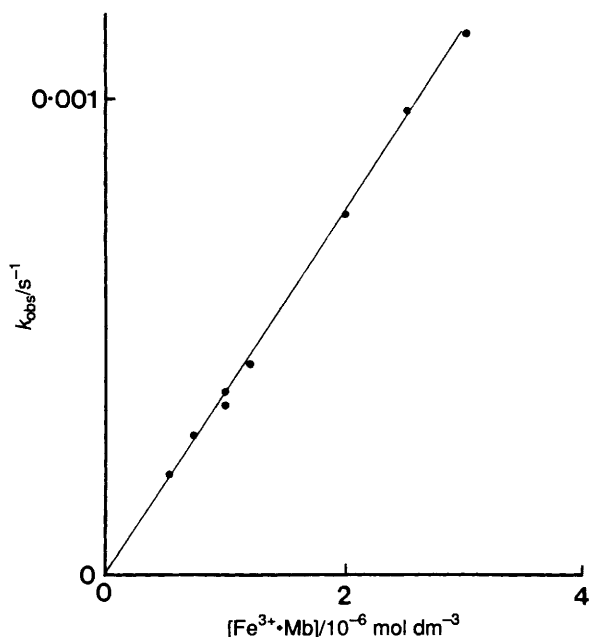


Fig. 3 Dependence of k_{obs} on $[\text{Fe}^{3+}\text{Mb}]$ under pseudo first-order conditions. $[\text{H}_2\text{O}_2] = 2 \times 10^{-5} \text{ mol dm}^{-3}$ (i.e. $K_{\text{m(app)}/30}$); $[\text{ABTS}] = 1.25 \times 10^{-3} \text{ mol dm}^{-3}$ the slope of the line $\equiv V_{\text{m}}/(K_{\text{m(app)}} \times [\text{Mb}]$, i.e. $390 (\pm 12) \text{ mol}^{-1} \text{ dm}^3 \text{ s}^{-1}$.

line dependences on $[\text{H}_2\text{O}_2]$ with intercept at $[\text{H}_2\text{O}_2] = k_0$.

(iii) The efficiency of ABTS^+ formation decreases with increasing $[\text{H}_2\text{O}_2]$.

(iv) Spectrophotometric titration of the HP:NHP complex with ABTS indicates formation of a 1:1 complex between the species [Fig. 4(a)].

(v) A plot of $k_0/[\text{HP:NHP}]$ vs. $[\text{ABTS}]$ [Fig. 4(b)]—where k_0 is the extrapolated pseudo first-order rate constant at $[\text{H}_2\text{O}_2] = 0$ —is of the inverse hyperbolic type, this is also consistent with formation of a 1:1 complex between HP:NHP and ABTS.⁴ In addition the concentration dependence of the Soret peak of the complex obeys Beer's Law accurately up to a concentration of $5 \times 10^{-6} \text{ mol dm}^{-3}$ indicating that the complex is monomeric in aqueous solution.

The effect of pH on the kinetics of H_2O_2 reduction for the HP:NHP and Fe^{3+}Mb catalysed processes

The pH variation of k_{obs} with $[\text{H}_2\text{O}_2]$ in the range $5.0 \leq \text{pH} \leq 8.75$ is shown for the HP:NHP complex in Fig. 5. At pH values ≥ 7.00 k_{obs} was evaluated from the full first-order curve, while at pH 6.00, 5.50 and 5.00, k_{obs} was calculated from the initial rates of ABTS formation obtained as described previously.⁴

Fig. 5 (inset) shows the variation of k_0 (the intercept at $[\text{H}_2\text{O}_2] = 0$) with pH, the solid line being the non-linear least-squares fit of the data assuming a single pH dependent equilibrium transition between a low- and high-pH form of the complex.

Increasing pH in the Fe^{3+}Mb catalysed system resulted in a decrease in k_0 which also appeared to follow a sigmoidal-type curve characteristic of a single pH dependent transition from a low to high pH form of the protein.

Fig. 6 shows the pH variation of the second-order rate constant k_2 , calculated from k_0 , after correcting for the activity of the low pH form of the HP:NHP complex to give $k_{2(\text{obs})}$, and then further correcting according to eqn. (2), which is derived on the assumption that the high pH form is a catalytically

$$k_2 = k_{2(\text{obs})} \{1 + K_a/[\text{H}^+]\} \quad (2)$$

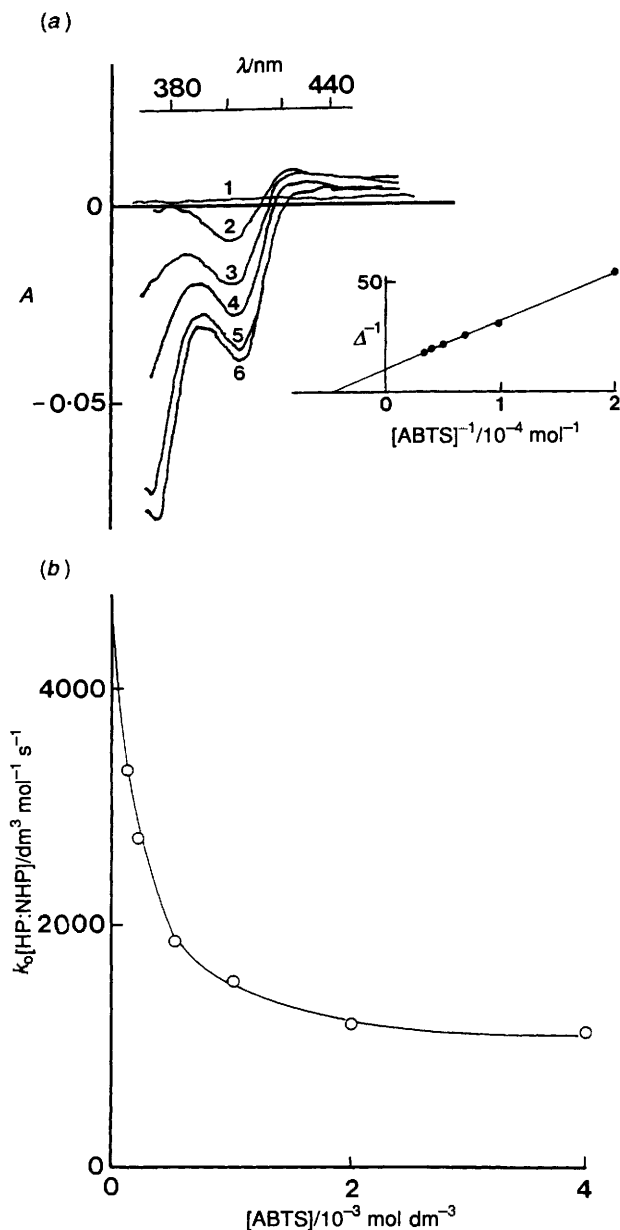


Fig. 4 (a) Spectrophotometric titration of the $[\text{HP:NHP}]$ complex with ABTS. The inset shows the double reciprocal plot of the data demonstrating a hyperbolic dependence of absorbance on $[\text{ABTS}]$. Fitting of the data to the Hill equation gave 'n' (the Hill coeff) = 1.02 (1:1 complex) with $K_d = (1.6 \pm 0.1) \times 10^{-4} \text{ mol dm}^{-3}$. Traces 1–6 are for $[\text{ABTS}] = 0, 0.05, 0.15, 0.2, 0.25, 0.3 \times 10^{-3} \text{ mol dm}^{-3}$, respectively; $\equiv (A_{420} - A_{402})$. The spectral trace at 0.10 mol dm^{-3} has been omitted from the figure to avoid overcrowding. (b) Variation of $k_0/[\text{HP:NHP}]$ with $[\text{ABTS}]$ demonstrating the existence of differing catalytic activity of the HP:NHP complex and the HP:NHP-ABTS complex. The limiting rate constants (k^*) given on fitting a hyperbolic equation to the data are (4520 ± 160) and $(910 \pm 120) \text{ dm}^3 \text{ mol}^{-1} \text{ s}^{-1}$ with $K_d = 0.19 (\pm 0.02) \times 10^{-3} \text{ mol dm}^{-3}$.

inactive hydroxo-complex—as found for Horseradish Peroxidase (HRP), Turnip Peroxidase (TRP), catalase^{12,13} and MP-8.¹⁴ K_a was calculated using the $\text{p}K_a$ value of 7.40 obtained from the inset to Fig. 5. The slope of the straight line in Fig. 6 is 1.02 ± 0.02 . As with MP-8¹⁴ this suggests that the complex reacts with the HO_2^- anion as well as the intact H_2O_2 moiety. Extrapolation to pH 11.8 ($\text{p}K_a$ of H_2O_2) gives—on the basis of this assumption—a pH independent value for k_2 of $(6.6 \pm 0.9) \times 10^7 \text{ mol}^{-1} \text{ dm}^3 \text{ s}^{-1}$.

Correction of the Fe^{3+}Mb data with the same assumption

and with pK_a taken to be 8.9, showed (Fig. 6) that k_2 is pH independent indicating that $Fe^{3+}Mb$ reacts only with H_2O_2 and not the HO_2^- anion in the pH range 5–9. The second-order rate constant found here ($390 \text{ dm}^3 \text{ mol}^{-1} \text{ s}^{-1}$) compares well with the value of $444 \text{ dm}^3 \text{ mol}^{-1} \text{ s}^{-1}$ quoted recently by Wazawa *et al.*¹⁵ for the interaction of H_2O_2 with $Fe^{3+}Mb$.

The effect of formate (HCO_2^-) and bromide (Br^-) ions on the efficiency (E , as defined in ref. 4) and pseudo first-order rate constants (k_{obs}) for the catalytic process

Fig. 7 (a/b) shows the effect of the powerful OH^\cdot scavengers Br^- and HCO_2^- (with Cl^- as reference ion) on both k_{obs} and

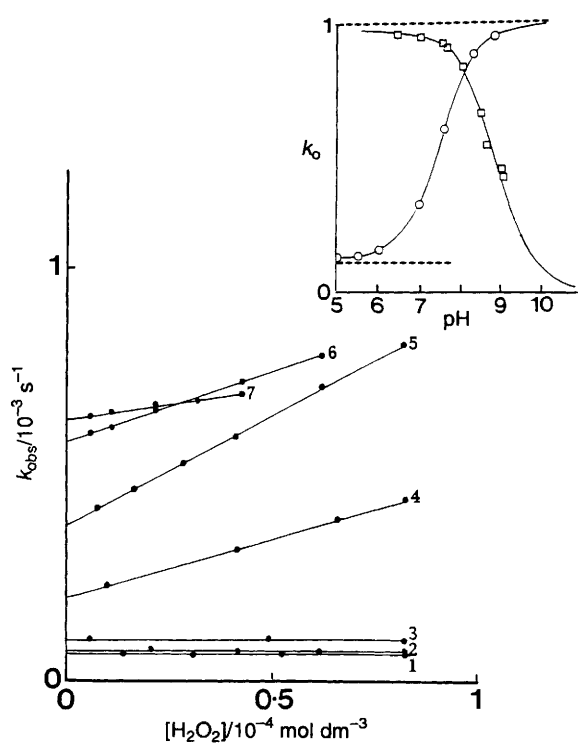


Fig. 5 pH Variation of k_{obs} with $[H_2O_2]$. $[ABTS] = 1 \times 10^{-3} \text{ mol dm}^{-3}$, $[HP:NHP] = 4.17 \times 10^{-7} \text{ mol dm}^{-3}$. Lines 1–7 correspond to pH values of 5.0, 5.5, 6.0, 7.0, 7.51, 8.25 and 8.75, respectively. The inset shows the normalized pH dependence of k_o , the $[H_2O_2]$ independent rate constant (\circ). Also included in the inset to the figure are values of the pH dependence of k_o for the $Fe^{3+}Mb$ catalysed process (\square).

E , for the $Fe^{3+}Mb$ catalysed peroxidasic reaction. Br^- and Cl^- have no significant effect on k_{obs} for the $Fe^{3+}Mb$ or the HP:NHP complex catalysed process. HCO_2^- is without effect on k_{obs} in the HP:NHP system but decreases k_{obs} in the $Fe^{3+}Mb$ catalysed system.

Br^- , Cl^- and HCO_2^- are without significant effect on E for the HP:NHP system. Cl^- is without effect on the $Fe^{3+}Mb$ system, increasing $[Br^-]$ however increases E to an apparent limit of $\approx 10\%$ while HCO_2^- significantly decreases E by approximately the same percentage.

Sequential efficiency studies of the $Fe^{3+}Mb$; HP:NHP and MP-8 catalysed system

If the catalytic process, carried out under strict pseudo first-order conditions, is allowed to proceed essentially to

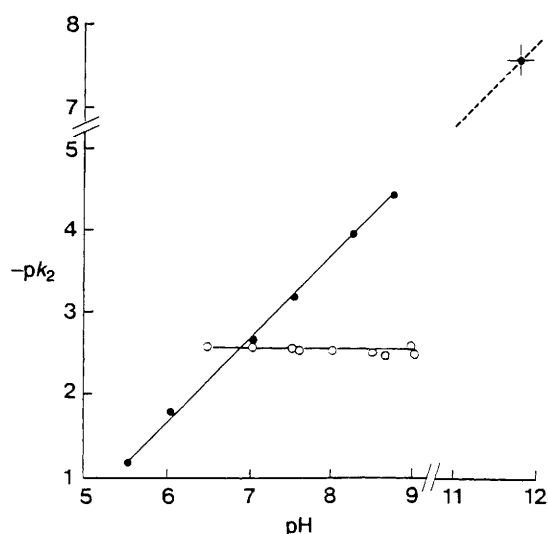


Fig. 6 Plot of the second order rate constant k_2 for HP:NHP (\bullet) and $Fe^{3+}Mb$ (\circ), after correction for (a) the low pH activity form in the case of the HP:NHP complex and (b) the formation of a catalytically inert hydroxo species (assuming $pK_a = 7.40$ and 8.9 , respectively). The slope of the line for HP:NHP is 1.02 ± 0.02 and extrapolation to pH 11.7 (the pK_a of H_2O_2) is shown, giving a value for the pH independent rate constant of $6.6 \times 10^7 \text{ dm}^3 \text{ mol}^{-1} \text{ s}^{-1}$. For $Fe^{3+}Mb$ the line is pH independent, the horizontal line shown corresponding to a k_2 value of $390 \text{ dm}^3 \text{ mol}^{-1} \text{ s}^{-1}$. (The highest pH result shown for $Fe^{3+}Mb$ is at 9.)

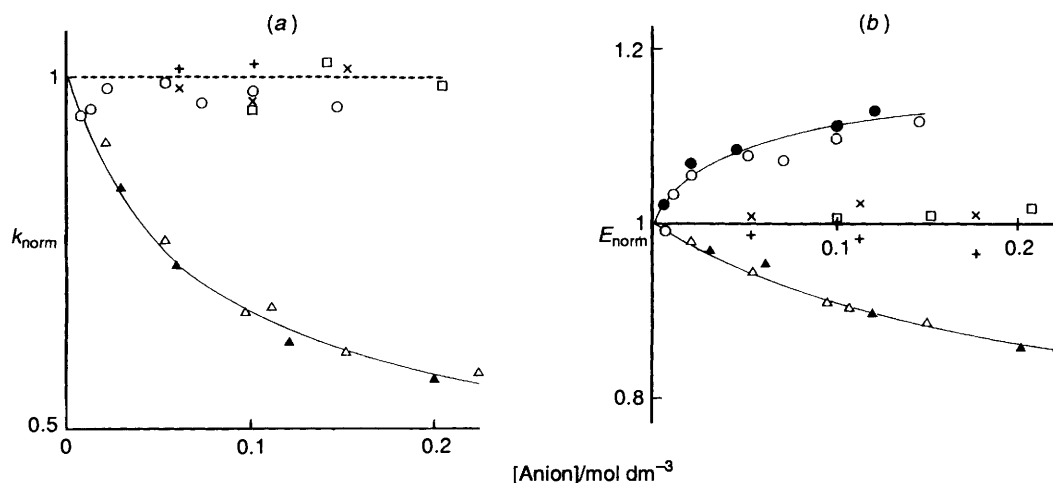


Fig. 7 (a), (b) Effect of OH^\cdot scavengers Br^- and HCO_2^- on $k_{obs(norm)}$ and $E_{(norm)}$ for the $Fe^{3+}Mb$ 'peroxidasic' system. (\square), Cl^- ; (\circ), Br^- ; (\triangle), HCO_2^- . The solid symbols are the results of repeat experiments where significant variation with anion concentration was found in the first experimental set. Results obtained for the HP:NHP system are shown for comparison; (+), Br^- ; and (\times), HCO_2^- , respectively.

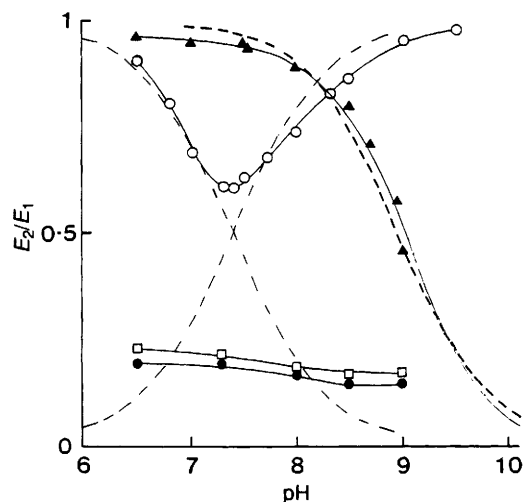


Fig. 8 pH Variation of E_2/E_1 for MP-8/11 (\square , \bullet); HP:NHP (\circ) complex and Fe^{3+}Mb (\blacktriangle). Dotted lines show relative concentrations of HP:NHP Met-80/aquo and hydroxo forms assuming $\text{p}K_a$ 7.4, and of $\text{Fe}^{3+}\text{Mb}\cdot\text{H}_2\text{O}$ assuming $\text{p}K_a$ 8.95.

completion ($> 6 \times t_2$) and further H_2O_2 is added to restore the initial concentration, then further catalytic formation of ABTS^{+} is observed indicating that viable, *i.e.* non-degraded catalyst, is present in the system. The extent of the second catalytic reaction is thus a measure of the extent of haem-degradation (also see Discussion) during catalytic cycling *i.e.* if identical efficiencies are obtained in sequential reactions, no catalyst degradation is occurring. Conversely, if no reaction is found in the second catalytic reaction then complete catalytic degradation has occurred during the first reaction.

Thus, the ratio E_2/E_1 (where $E_1 \equiv$ efficiency of the first catalytic reaction and $E_2 \equiv$ efficiency of the repeat catalytic reaction) provides a convenient dimensionless indicator of haem degradation, independent of the between-catalyst variation in the absolute efficiency of ABTS trapping with pH. The variation of E_2/E_1 with pH for MP-8/MP-11, HP:NHP and Fe^{3+}Mb is shown in Fig. 8.

When three sequential reactions were carried out (results not shown) the relative change in E was found to be approximately constant, *i.e.* the efficiency drops by approximately the same amount each catalytic cycle; $E_2/E_1 \approx E_3/E_2$.

Complex formation and active site accessibility

As with MP-8, spectrophotometric titration of the HP:NHP complex with ABTS suggests the formation of a 1:1 complex between the reducing substrate and protein [Fig. 4(a)]. ABTS is a relatively large molecule, it therefore follows that access to the haem must be relatively unhindered, a conclusion which is supported by the fact that k^* [defined in ref. 4 and eqn. (3)—Discussion this paper] is found to be $4520 \text{ dm}^3 \text{ mol}^{-1} \text{ s}^{-1}$ only slightly lower than the values of 4780 and $5290 \text{ dm}^3 \text{ mol}^{-1} \text{ s}^{-1}$ previously reported for MP-8.^{4,14} The low pH form of the HP:NHP complex has an intact haem crevice, as evidenced by a 695 nm absorption band. However this low pH form still retains peroxidasic catalytic activity suggesting that the association of the sixth ligand (Met-80) with the iron is considerably weaker than in cytochrome *c* which is effectively catalytically inactive, thus the ligand can be displaced by the $\text{H}_2\text{O}_2\text{-HO}_2^-$ to form a catalytically competent Michaelian complex, we consider that the sixth coordination position in this complex is probably shared between Met-80 and H_2O .

Discussion

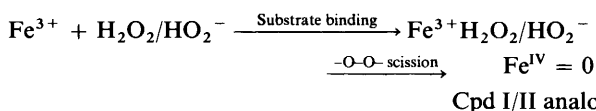
General comments

Previous studies of the system MP-8- H_2O_2 -ABTS under strict pseudo first-order non-saturation conditions at pH 7.00 and 25 °C led us to propose⁴ the existence of two parallel 'peroxidasic' catalytic pathways, the first of which utilized MP-8 as catalyst, the second involving an MP-8-ABTS complex of lower catalytic activity than MP-8 but more resistant to H_2O_2 mediated oxidative degradation than MP-8 alone. Kinetic characterization of the three-parallel-path reaction network led to the master eqn. (3) for k_{obs} .⁴ Although discussed in detail in

$$k_{\text{obs}} = [\text{MP-8}] \left\{ k^* + \frac{a[\text{H}_2\text{O}_2]}{b + [\text{ABTS}]} - \frac{c[\text{ABTS}]}{d + [\text{ABTS}]} \right\} \quad (3)$$

ref. 4 it is useful to recap briefly the meaning of the individual terms in eqn. (3). In eqn. (3) k^* is the second-order rate constant found for the 'peroxidasic' catalytic cycle of the haempeptide alone. The term $\{a[\text{H}_2\text{O}_2]/(b + [\text{ABTS}])\}$ refers to the H_2O_2 dependent haem degradative pathway in which protection is afforded the haem by complex formation with ABTS. The term $\{-c[\text{ABTS}]/(d + [\text{ABTS}])\}$ reflects the transition from the uncomplexed haem to the haem-ABTS complex which possessed a lower catalytic activity, *i.e.* the second peroxidasic pathway. Values for the limiting constants of eqn. (3) at pH 7.00 are collected in Table 1 for MP-8, HP:NHP and the Fe^{3+}Mb system, the data for MP-8 being taken from ref. 4, while those for Fe^{3+}Mb and HP:NHP are evaluated in the present study, reported here. In the case of the myoglobin system at pH 7.00 no significant degradative path was found and no complex formation was observed, we thus utilize only the limiting parameter k^* . The Table also includes values for the kinetic $\text{p}K_a$ s observed for the systems as well as the association/dissociation constants for ABTS complex formation.

Several points of note arise on comparison of the constants in Table 1. Firstly, the primary catalytic constant k^* is essentially the same for MP-8 and HP:NHP, and agrees well with the value obtained by Baldwin *et al.* for MP-8 using guaiacol as reducing substrate.¹⁴ This observation, namely that k^* is independent of the nature of the reducing substrate, supports the identification of the binding/catalytic stage of the reaction as the rate determining stage of the reaction. The abstraction



steps, where the reducing substrate accepts oxidising equivalents from the hypervalent Cpd I and II oxo-iron(IV) porphyrin analogues are known to be very fast in comparison with the values of k^* obtained in this and previous work.⁴ Secondly, the value of a the second-order 'degradative' rate constant for the HP:NHP system is only 6% of the value found for the MP-8 system. This suggests that the haem in the complex is far less susceptible to oxidative degradation than in the microperoxidase (MP-8 and MP-11) where the distal haem face is fully exposed to bulk solvent. In myoglobin haem degradation is virtually absent at pH 7.0.

Both spectrophotometric and kinetic data indicate that ABTS forms a 1:1 complex with both MP-8 and the HP:NHP complex. Since this involves only a change in intensity in the Soret region of the haem, and not in λ_{max} , we suggest that the complex is formed by non-polar interaction with the tetrapyrrole ring system as suggested for the interaction of MP-8 with human placental glutathione S-Transferase.¹⁶ The

Table 1 Kinetic and equilibrium parameters [eqn. (3)] for the MP-8; HP:NHP and Fe³⁺Mb catalysed 'peroxidasic' reduction of H₂O₂ using ABTS as reducing substrate. pH 7.00; $\mu = 0.1$; $T = 25^\circ\text{C}$ ^a

	k^*/dm^3 $\text{mol}^{-1} \text{s}^{-1}$	$a/10^{-5} \text{dm}^3$ $\text{mol}^{-1} \text{s}^{-1}$	$b/10^4 \text{mol dm}^{-3}$	$c/\text{dm}^3 \text{mol}^{-1} \text{s}^{-1}$	$d/10^3 \text{mol dm}^{-3}$	$K_d/10^3 \text{mol dm}^{-3}$	$\text{p}K_a$
MP-8 ⁴	4778 (87)	1.49 (0.03)	2.82 (0.07)	3700 (100)	1.08 (0.08)	0.9 (0.05)	8.2 (0.1) ^b
HP:NHP	4520 (160)	0.086 (0.01)	2.45 (0.11)	3610 (140)	0.19 (0.02)	0.16 (0.04)	7.4 (0.05)
Fe ³⁺ Mb	390 (12)						8.9 (0.1)

^a In parentheses are one std. dev. in the mean; K_d obtained from spectrophotometric titration of MP-8 and HP:NHP with ABTS; $\text{p}K_a$ obtained from the variation of k_o (inset Fig. 5) with pH. ^b Ref. 16.

lower dissociation constant found for the HP:NHP complex in which the tetrapyrrole ring is shielded from bulk solvent relative to MP-8, supports this conclusion. The lack of complex formation in the case of Fe³⁺Mb, however, does not necessarily imply that the haem binding cleft is highly polar, an alternative explanation being that steric factors prevent planar π - π hydrophobic interaction between ABTS and the tetrapyrrole ring system.

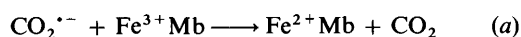
A further point of relevance is that if such hydrophobic complexes are formed between the reducing substrate and the tetrapyrrole ring system of the haem, then it is entirely feasible that such complexes could either stabilize the system toward oxidative degradation by H₂O₂⁴ or depending on the nature of the substrate (if for example it forms highly reactive radical species) facilitate haem degradation in the system as proposed by Cunningham *et al.*¹⁷

Effect of formate and bromide ions on ABTS^{•+} formation

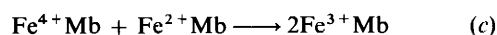
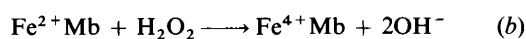
The limiting (maximum) efficiency for ABTS^{•+} formation in the Fe³⁺Mb system is 140% at pH 7.0. This fact alone indicates that ABTS must have some degree of access to the Fe^{1V} = 0 species in the protein and is not merely reacting with a relatively accessible tyrosine phenoxyl radical on the surface of the protein. Ortiz de Mellano⁶ has commented specifically on the fact that, despite the apparent (from the crystal structure) lack of an access channel to the haem, relatively large substrates are able to reach the iron coordination site of Fe³⁺Mb. However the apparent inability of ABTS to form a complex with Fe³⁺Mb indicates that ABTS cannot easily approach the tetrapyrrole ring system to form planar π - π complexes.

The limiting increase of $\approx 10\%$ in the reaction efficiency in the presence of Br⁻ ion for the Fe³⁺Mb process can be interpreted using the rationale of Rush and Koppenol⁸ as evidence for the formation of OH[•] from homolytic scission of the dioxygen bond in an Fe³⁺Mb-H₂O₂/HO₂⁻ Michaelis type complex prior to formation of a protein radical species. Since the Br⁻ ion reacts subsequent to the rate determining step of the reaction it would not be expected to affect k_{obs} , as is indeed observed.

The formate ion reacts with the OH[•] radical to give rise to the carbon dioxide radical anion CO₂^{•-}—a strong reducing agent. This would result in the observed efficiency of ABTS^{•+} formation, from reaction with OH[•], decreasing. Furthermore the CO₂^{•-} radical anion formed would be well positioned to reduce the Fe³⁺Mb resulting from the catalytic process according to (a)⁸ the Fe²⁺Mb can then act as a further non-



ABTS^{•+} forming sink for H₂O₂ according to (b) and (c).¹⁵



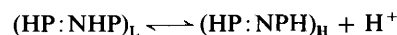
Thus, the steady-state concentration of Fe³⁺Mb available for reaction in the rate determining step of the 'peroxidasic' cycle

could be reduced resulting in a decrease in k_{obs} with increasing formate ion concentration as found [Fig. 7(a)].

The above interpretation of the Fe³⁺Mb-H₂O₂ reaction is in contrast to that of Davies and co-workers who,¹⁸ on the basis of stopped flow EPR spectroscopy and radical scavenger effects conclude that the formation of the protein radical species occurs *via* electron transfer from an oxo-iron(IV) porphyrin π cation radical species (cpd I analogue) and not by intermediacy of an OH[•] (or other oxo) species. A number of points are relevant, firstly their reactions were carried out under conditions of approximately equal Fe³⁺Mb and H₂O₂ concentration under non-catalytic (*i.e.* absence of reducing substrate) conditions, whereas the present system was investigated under conditions of catalytic cycling ($[\text{H}_2\text{O}_2] \gg [\text{Fe}^{3+}\text{Mb}]$) in the presence of ABTS. Secondly abstraction of the oxidising equivalents by ABTS with efficiency 140% (*i.e.* >1 oxidising equivalents scavenged) indicates that the ABTS must have some access to the region of the haem iron and is not scavenging merely the exposed protein radical. Thirdly the OH[•] scavengers used here HCO₂⁻ and particularly Br⁻ are considerably smaller than those used by Davies *et al.* and would have more facile access to oxidant species formed in the region of the haem iron. Finally the reactions of H₂O₂ with liganded iron are multiple and extremely complex,⁸ and we consider it feasible that a protein not specifically evolved to metabolise H₂O₂ could exhibit a variety of mechanisms by which a protein radical species is formed, especially under the concentration conditions used in catalytic studies.

Effect of pH on catalysis and haem degradation

Increasing the pH from 5.0 to 8.75 results in an increase in k_o (Fig. 5). The pH dependence of k_o is consistent with a simple pH dependent equilibrium between a low pH form and high pH form of the complex. The kinetic $\text{p}K_a$ of the equilibrium, 7.40,



is almost identical to the value of 7.35 obtained spectrophotometrically by following the disappearance of the 695 nm band of the complex.¹⁰ This $\text{p}K_a$ corresponds to the change from spectral state III to spectral state IV of ferricytochrome c and accompanies a ligand change at the sixth position. It is not known from spectral studies which species replaces the Met-80, however the kinetic studies reported here suggest the possibility, by analogy with MP-8,¹⁴ that the transition involves replacement of the sixth ligand to give a catalytically inert species. The linear dependence of $\log k_2$ (after correction for formation of the catalytically inert complex) with slope ≈ 1 indicates that the reactive form of the substrate at high pH is the HO₂⁻ anion. The pH independent value for reaction of HO₂⁻ anion with (HP:NHP)_L, k_2 ($6.6 \times 10^7 \text{dm}^3 \text{mol}^{-1} \text{s}^{-1}$) is in good agreement with the value of $1.25 \times 10^8 \text{dm}^3 \text{mol}^{-1} \text{s}^{-1}$ found for reaction of cytochrome c peroxidase¹⁹ and the value of $\approx 10^7 \text{dm}^3 \text{mol}^{-1} \text{s}^{-1}$ for reaction of horseradish peroxidase with H₂O₂.²⁰

A further point is that the HP:NHP complex possesses a

much reduced, but significant, low pH limiting catalytic activity with limiting $k \approx 200 \text{ dm}^3 \text{ mol}^{-1} \text{ s}^{-1}$, close to low pH value of $\approx 400 \text{ dm}^3 \text{ mol}^{-1} \text{ s}^{-1}$ found for Fe^{3+}Mb . This low pH catalysis can only result from reaction of intact H_2O_2 , not the HO_2^- species, with the iron porphyrin and suggests that the low pH, low activity form of the complex is the HP:NHP- H_2O_2 adduct. These observations support two possible reaction pathways for redox catalysis of H_2O_2 reduction by haem protein enzymes. The first involves reaction of the haem iron with the HO_2^- anion. In the peroxidases, reaction *via* this pathway is facilitated by a relatively polar haem environment combined with the ability of the protein to bind H_2O_2 as HO_2^- and H^+ at catalytically useful rates at neutral pH.

The second involves reaction of the intact H_2O_2 moiety with the iron centre of the haemprotein catalyst. Examination of published pH *vs.* k_2 data for MP-8¹⁴ indicate a low pH limit of $\approx 300 \text{ dm}^3 \text{ mol}^{-1} \text{ s}^{-1}$. The fact that the low pH second-order rate constant appears independent of the mechanism of -O-O- bond scission (heterolytic for MP-8 and NP:NHP; possible parallel homo- and hetero-lytic for Fe^{3+}Mb) suggests that the rate determining step in the reaction is the $\text{H}_2\text{O}_2/\text{HO}_2^-$ binding step. This conclusion is in agreement with that reached by Baldwin *et al.*¹⁴ for reaction of MP-8 with H_2O_2 but is in apparent contradiction to the hyperbolic kinetics exhibited by Fe^{3+}Mb (Fig. 1) which superficially suggest -O-O- bond scission as the rate determining stage. In this respect Laidler²¹ has emphasised that for a simple one-intermediate mechanism of the type relevant to the rate determining part of the overall reaction scheme, the steady state criteria can *always* be satisfied—subject to solubility limitations—by making the non-catalytic species (in this case H_2O_2) concentration very much greater than that of the catalytic species.

Haem degradation during catalysis

As shown in Fig. 2 the k_{obs} *vs.* $[\text{H}_2\text{O}_2]$ plots for Fe^{3+}Mb show the negative initial slope expected in the case of a catalytic system following Michaelian kinetics in the absence of catalyst degradation.¹¹ In contrast the plots of k_{obs} *vs.* $[\text{H}_2\text{O}_2]$ for the HP:NHP system, Fig. 5, show an approximately zero slope at low pH increasing to a maximum positive slope at pH ≈ 7.5 followed by a decreasing positive slope at high pH. This implies relatively little catalytic haem degradation at low and high pH with maximum degradation at pH ≈ 7.5 . These observations can be compared to those obtained for MP-8⁴ (and MP-11—PAA, unpublished results) where a significant positive slope is found for the k_{obs} *vs.* $[\text{H}_2\text{O}_2]$ plots with a tendency to increase slightly with increasing pH, suggesting extensive catalyst degradation for the small haempeptides over the entire pH range studied.

Data derived from the sequential efficiency studies (Fig. 8) are informative regarding the factors mediating haem degradation in haemproteins, however, before considering these observations it is useful to discuss the factors which affect the observed efficiency of the reaction,⁴ and the relevance of the ratio E_2/E_1 to haem degradation.

H_2O_2 can react with the catalytic system *via* three main routes. Firstly, reaction to form a cpd I intermediate can proceed either as in peroxidase, *i.e.* by reaction with ABTS removing one H_2O_2 per catalytic cycle, or as in catalase where reaction occurs with a further H_2O_2 to give catalyst H_2O and O_2 , the catalase reaction removing $2\text{H}_2\text{O}_2$ per catalytic cycle.

Thirdly, H_2O_2 can react non-catalytically with the iron porphyrin at multiple sites on the tetrapyrrole macrocycle, the first of these inactivating the catalyst, subsequent reactions continuing to divert H_2O_2 from the ABTS^{+} forming pathway.

The ratio E_2/E_1 for Fe^{3+}Mb follows a simple decreasing sigmoidal curve (Fig. 8) with $\text{p}K_a = 9.0 \pm 0.1$ (Fig. 8). This $\text{p}K_a$ corresponds closely with the spectrophotometric 'alkaline'

transition $\text{p}K_a$ (8.93; 8.99) for Fe^{3+}Mb in which the sixth ligand of the iron changes from H_2O to OH^- ,^{22,23} and the value of 8.9 ± 0.1 found kinetically (inset to Fig. 5), the hydroxo species being catalytically inactive (from variation of k_0 with pH—inset Fig. 5 and results of other workers on HRP, TRP, catalase and MP-8).^{12,13} Thus, for both Fe^{3+}Mb and the HP:NHP complex the low pH form is stable to H_2O_2 mediated oxidative degradation, however the decrease in E_2/E_1 as the pH increases closely mirrors (initially for the HP:NHP) the increase in the catalytically inactive hydroxo-species, thus the high pH hydroxo form is the species susceptible to irreversible degradation. The apparent increasing stability of the HP:NHP complex (from ratio E_2/E_1 , Fig. 8) as the pH increases above 7.4 could be a consequence of the fact that reaction of the aquo complex with HO_2^- is very much faster than with H_2O_2 ($k_{\text{HO}_2^-}/k_{\text{H}_2\text{O}_2} \approx 3 \times 10^5$). Thus, while the flux of H_2O_2 through the degradative pathway remains constant, that through the catalytic pathway is greatly increased, this results in a decreased probability of degradation on each approach of a peroxo species to the haem. The essentially invariant low ratio of E_2/E_1 observed for MP-8/MP-11 arises from the fact that no steric protection is afforded the distal face of the haem in these complexes.

The invariance of the corrected k with pH for Fe^{3+}Mb (Fig. 6) indicates that aquo Fe^{3+}Mb reacts only with H_2O_2 and not with the HO_2^- anion in the pH range studied here. This conclusion appears to contradict the suggestions of other authors²⁴ who consider that reaction of Fe^{3+}Mb occurs with both H_2O_2 and HO_2^- (in a system which does not use ABTS as reducing substrate). While we also find that, as the pH increases to above 10 in the Fe^{3+}Mb system, the value of k_0 begins to increase (results not shown), we feel that such observations should be interpreted with caution since it is well known that Fe^{3+}Mb dissociates into Ferriprotoporphyrin IX and apo Mb at extremes of pH. Thus, the existence of extremely low concentrations of Ferriprotoporphyrin IX, which reacts with HO_2^- anion could lead to the erroneous conclusion that Fe^{3+}Mb itself was reacting with HO_2^- —this topic is currently the subject of further investigation.

The lack of reaction of Fe^{3+}Mb with HO_2^- below pH 9 could also account for the inability of Fe^{3+}Mb to utilize kinetic protection—as postulated for the HP:NHP complex—against oxidative haem degradation (Fig. 8).

The studies reported here can thus be interpreted to support two ways in which the haem is protected against oxidative degradation firstly by the protein envelope, *i.e.* steric protection and secondly kinetic protection by the increased reactivity of Fe^{3+} with HO_2^- , in addition some insight is provided into factors in the environment of the haem which lead to either homolytic or heterolytic scission of dioxygen being favoured. It is well known²⁵ that homolysis is favoured for cleavage of non-polar symmetrical covalent bonds in non-polar environments, while heterolysis is favoured for the cleavage of highly polar unsymmetrical bonds in polar environments. At low pH aquo Fe^{3+}Mb (in which the haem is situated in a 'hydrophobic cleft' in the protein²⁶) reacts with H_2O_2 , the combination of substrate symmetry and the hydrophobic environment being favourable to homolysis of the -O-O- bond, the effect of Br^- and HCO_2^- ions on the reaction as reported here do indeed suggest some homolytic component for the reaction. In contrast MP-8 is unaffected by Br^- and HCO_2^- indicating that the highly polar environment of the haem distal face directs toward heterolysis in this system.⁴ This suggests that the environment of the haem in the HP:NHP complex is significantly more polar than that of Fe^{3+}Mb resulting in heterolysis being favoured over homolysis in this complex (no significant effects of Br^- or HCO_2^-). This mechanistic assessment of haem distal face polarity in HP:NHP is also in accord with that deduced by

Wallace and Proudfoot¹⁰ from the biological activity and pK_a s found for the alkaline transition of these complexes relative to cytochrome c. Clearly in the case of MP-8 and the HP:NHP complex, reaction *via* a heterolytic pathway will be even further favoured on replacement of symmetrical H_2O_2 with the polar, asymmetrical HO_2^- anion.

In conclusion we would note the recent studies of Van Wart and co-workers,^{27,28} who used low temperature rapid scan kinetics to demonstrate the intermediacy of a 'cpd 0' subsequent to the Michaelis complex and prior to 'cpd 1' formation, for the reaction of H_2O_2 with acetyl MP-8 and horseradish peroxidase. This result may have important implications regarding the nature of the peroxo species interacting with haem iron, since it raises the possibility that even in horseradish peroxidase the peroxide may bind initially as H_2O_2 and subsequently dissociates to $Fe^{3+} \cdot HO_2^- + H^+$. The latter asymmetric charged species subsequently undergoing heterolysis in the polar haem environment to give cpd I, *etc.*

Experimental

Ferrimyoglobin (ex Sigma Chemical Corporation) was further purified by the recrystallization procedure of Yonetani and Schleyer¹⁹ to give a product with purity index (E_{409}/E_{280}) 5.79 at pH 5 and 23 °C. The HP:NHP complex was prepared and purified from horse heart cytochrome c (Sigma Chemical Corporation) by the HCl digestion procedure of Wallace and Proudfoot.¹⁰ The purity of the product was assessed by reverse phase HPLC using an analytical C18 Vydac column with 0.1% TFA and 0.1% TFA-acetonitrile as eluents. The procedure was monitored spectrophotometrically at 230 nm (peptide) and 396 nm (haem) and indicated two peptides in a 1:1 ratio—a non-haempeptide (51–104) and haem peptide (1–50). The purity of the complex was estimated greater than 95%, the product being essentially free of cytochrome c. Following lyophilization the amorphous product was stored dry under N_2 at –10 °C. Catalytic reactions reported here utilizing the pure haem undecapeptide (MP-11), prepared from cytochrome c as previously described,²⁹ were carried out at [MP-11] of 5×10^{-8} mol dm^{-3} in order to minimise possible haem peptide aggregation effects. Diluted stock solutions of the MP-11 were allowed to stand at room temperature for 30 min prior to use to ensure that disaggregation of the catalyst was complete. For kinetic runs at pH values > 8.50, the buffer was 0.01 mol dm^{-3} Tris, with $\mu = 0.1$ (KCl). All other materials methods and instrumentation here used have been fully described in a previous publication.^{†4}

† Eqn. (3) in ref. 4 should read $Abs = A + B(\exp^{-k_{obs}t})$ and not $Abs = A + B^{-k_{obs}t}$ as in the reference.

Acknowledgements

The authors are indebted to Dr D. A. Baldwin for his critical reading of the manuscript and many helpful suggestions and to Lucille Odes for manuscript preparation.

References

- R. D. Jones, D. A. Summerville and F. Basolo, *Chem. Rev. (USA)*, 1979, **79**, 139.
- P. A. Adams, in *Peroxidases in Chemistry and Biology*, vol. II, eds. J. Everse, K. E. Everse and M. B. Grisham, CRC Press, Boca Raton, 1991, p. 171.
- C. Adams and P. A. Adams, *J. Inorg. Biochem.*, 1992, **45**, 47.
- P. A. Adams, *J. Chem. Soc., Perkin Trans. 2*, 1990, 1407.
- P. A. Adams and R. D. Goold, *J. Chem. Soc., Faraday Trans.*, 1990, **86**, 1803.
- P. R. Ortiz de Montellano, *Acc. Chem. Res.*, 1987, **20**, 289.
- P. George, *Adv. Catal.*, 1952, **4**, 367.
- J. D. Rush and W. H. Koppenol, *J. Am. Chem. Soc.*, 1988, **110**, 4957.
- A. E. I. Proudfoot and C. J. A. Wallace, *Biochem. J.*, 1987, **248**, 965.
- C. J. A. Wallace and A. E. I. Proudfoot, *Biochem. J.*, 1987, **245**, 773.
- P. A. Adams, *Int. J. Biochem.*, 1977, **8**, 499.
- J. Turner and D. E. Reed, *Biochim. Biophys. Acta*, 1984, **789**, 80.
- P. Jones and I. Wilson, in *Metals and Ions in Biological Systems*, ed. H. Siegel, Marcel Dekker, New York, 1978, p. 186.
- D. A. Baldwin, H. M. Marques and J. M. Pratt, *J. Inorg. Biochem.*, 1987, **30**, 203.
- T. Wazawa, A. Matsuoka, G. Tajima, Y. Sugawara, K. Nakamura and K. Shikama, *Biophys. J.*, 1992, **63**, 544.
- P. A. Adams and R. D. Goold, *J. Chem. Soc., Faraday Trans.*, 1990, **86**, 1797.
- I. D. Cunningham, J. L. Bachelor and J. M. Pratt, *J. Chem. Soc., Perkin Trans. 2*, 1991, 1839.
- M. J. Davies and A. Puppo, *Biochem. J.*, 1992, **281**, 197.
- T. Yonetani and H. Schleyer, *J. Biol. Chem.*, 1967, **242**, 1974.
- H. B. Dunford and W. D. Hewson, *Biochemistry*, 1977, **16**, 2949.
- K. J. Laidler and P. S. Bunting, in *The Chemical Basis of Enzyme Action*, Clarendon Press, Oxford, 1973, pp. 73–74.
- M. Brumori, G. Amiconi, E. Antonini, J. Wyman, R. Zito and A. Rossi Fanelli, *Biochim. Biophys. Acta*, 1968, **154**, 315.
- P. George and G. I. H. Hanania, *Biochem. J.*, 1952, **52**, 517.
- J. L. Bachelor, I. D. Cunningham, V. L. Hughes and J. M. Pratt, Abstracts, *Fifth International Conference on Bioinorganic Chemistry*, University of Oxford, August 1991, Abstract No. F074.
- E. M. Arnett, K. Amarnath, N.-G. Harvey and J. P. Cheng, *Science*, 1990, **247**, 423.
- E. Antonini and M. Brunori, in *Hemoglobin and Myoglobin in their Reactions with Ligands*, Frontiers of Biology, eds. A. Neuberger and E. L. Tatum, North Holland, Amsterdam, 1971, vol. 21, p. 86.
- J. S. Wang, H. K. Baek and H. E. Van Wart, *Biochem. Biophys. Res. Commun.*, 1991, **179**, 1320.
- H. K. Baek and H. E. Van Wart, *Biochemistry*, 1989, **28**, 5714.
- P. A. Adams, M. P. Byfield, R. D. Goold and A. E. Thumser, *J. Inorg. Biochem.*, 1989, **37**, 55.

Paper 4/07868C

Received 29th December 1994

Accepted 18th April 1995